THE JOURNAL OF BIOLOGICAL CHEMISTRY
Vol. 276, No. 29, Issue of July 20, pp. 27090–27097, 2001

Printed in U.S.A.

Laminin-10/11 and Fibronectin Differentially Regulate Integrin-dependent Rho and Rac Activation via p130^{Cas}-CrkII-DOCK180 Pathway*

Received for publication, March 14, 2001, and in revised form, May 10, 2001
Published, JBC Papers in Press, May 21, 2001, DOI 10.1074/jbc.M102284200

Jianguo Gu, Yasuhiro Sumida, Noriko Sanzen, and Kiyotoshi Sekiguchi‡

From the Division of Protein Chemistry, Institute for Protein Research, Osaka University, 3-2 Yamadaoka, Suita, Osaka 565-0871, Japan

The α_5 chain-containing laminin isoforms, laminins-10 and -11 (laminin-10/11), are the major components of the basement membrane, having potent cell-adhesive activity. We examined the cell-adhesive and integrin-mediated signaling activities of laminin-10/11 in comparison to fibronectin, the best characterized extracellular adhesive ligand. We found that laminin-10/11 are more active than fibronectin in promoting cell migration and preferentially activate Rac, not Rho, via the p130^{Cas}-CrkII-DOCK180 pathway. Cells adhering to fibronectin develop stress fibers and focal contacts, whereas cells adhering to laminin-10/11 do not, consistent with the high cell migration-promoting activity of laminin-10/11. Pull-down assays of GTP-loaded Rac and Rho demonstrated the preferential activation of Rac on laminin-10/11, in contrast to the activation of Rho on fibronectin. Activation of Rac by laminin-10/11 was associated with the phosphorylation of p130^{Cas} and an increased formation of a p130^{Cas}-CrkII-DOCK180 complex. Cell migration on laminin-10/11 was suppressed by the expression of either a dominant-negative Rac or CrkII mutants defective in p130^{Cas} or DOCK180 binding. This is the first report demonstrating a distinct activation of Rho family GTPases resulting from adhesion to different extracellular ligands.

Many cellular processes, such as growth, survival, and migration, require both soluble growth factors and integrin-mediated adhesion to the extracellular matrix (ECM).[1] Growth factor-induced signaling occurs within integrin-containing adhesion complexes (1, 2), assembly of which is regulated by the Rho family of GTPases. Activation of Rho induces the bundling of actin filaments into stress fibers and the clustering of integrins into focal contacts; activation of Cdc42 or Rac results in the formation of long, thin actin-containing extensions called filopodia and curtain-like extensions called lamellipodia, respectively (3).

The ligation of integrins triggers a multitude of signaling events, including activation of tyrosine kinases and subsequent phosphorylation of multiple cellular proteins such as focal adhesion kinase (FAK), p130^{Cas}, and paxillin. This cascade leads to the formation of signaling complexes by the coupling of signaling molecules with adaptor proteins containing SH2 and/or phosphotyrosine binding domains (1, 2). FAK plays a central role in integrin-mediated signal transduction through its association with Src family kinases, p130^{Cas}, Shc, Grb2, and phosphatidylinositol 3-kinase, leading to activation of the mitogen-activated protein kinase pathways (4). p130^{Cas} couples to FAK through an SH3 domain and to CrkII through a tyrosine-phosphorylated substrate domain. The p130^{Cas}-CrkII complex has been shown to serve as a molecular switch regulating integrin-mediated cell spreading and migration over an ECM-coated substratum through coupling with DOCK180, a guanine nucleotide exchange factor for Rac (5–7). Src family kinases are the major protein tyrosine kinases that phosphorylate FAK, p130^{Cas}, and other signaling proteins; tyrosine phosphorylation of these proteins is eliminated in cells with the triple mutation of the Src, Yes, and Fyn kinases (8).

There are more than 20 different integrin types, each having distinct ligand binding specificities. Gene knockout studies demonstrate that different integrin types have unique, irreplaceable functions, vascular defects in α_5 integrin-null mice and epithelial defects in α_3 or α_6 integrin-null mice (9). Nevertheless, most studies of integrin-mediated signaling events have been performed on cells adhering to fibronectin (FN) through $\alpha_5\beta_1$ integrin. The signaling events transduced by other integrin types remain unclear, particularly those containing α_3- or α_6-subunits that bind to laminins. In addition, it is also not known how these signals differ from those transduced by $\alpha_5\beta_1$ integrin.

Laminins are the major components of the basement membrane. Cells bind directly to laminins via a subset of integrins and other non-integrin-type receptors, such as dystroglycans. All laminins are composed of an α, β, and γ chain. At least 12 members of the laminin family have been identified, each composed of a distinct combination of heterotrimers (10–12). Of particular interest are those containing α_5 chain, as embryos lacking the laminin α_5 chain die late in embryogenesis without anterior neural tube closure or digit septation (13). The laminin α_5 gene is expressed in fetal and adult tissues, including the kidney, lung, skeletal muscle, skin, and intestine (14, 15). These results suggest the α_5-containing laminins, laminin-10 ($\alpha_5\beta_1\gamma_1$) and laminin-11 ($\alpha_5\beta_2\gamma_1$), have important roles in de-

* This work was supported by Special Coordination Funds from the Science and Technology Agencies of Japan, grants-in-aid from the Ministry of Education, Science, Sports, and Culture of Japan, and the Uehara Memorial Foundation. The costs of publication of this article were defrayed in part by the payment of page charges. This article must therefore be hereby marked "*advertisement*" in accordance with 18 U.S.C. Section 1734 solely to indicate this fact.

‡ To whom correspondence should be addressed: Institute for Protein Research, Osaka University, 3-2 Yamadaoka, Suita, Osaka 565-0871, Japan. Tel.: 81-6-6879-8617; Fax: 81-6-6879-8619; E-mail: sekiguch@protein.osaka-u.ac.jp.

[1] The abbreviations used are: ECM, extracellular matrix; FAK, focal adhesion kinase; FN, fibronectin; LN-10/11, laminins-10/11; DMEM, Dulbecco's modified Eagle's medium; FBS, fetal bovine serum; GST-RB, glutathione *S*-transferase to the Rho-binding domain of Rho-kinase; GST-CRIB, glutathione *S*-transferase to the Cdc42/Rac-interactive-binding domain of PAK1; PBS, phosphate-buffered saline; BSA, bovine serum albumin; mAb, monoclonal antibody; FITC, fluorescein isothiocyanate.

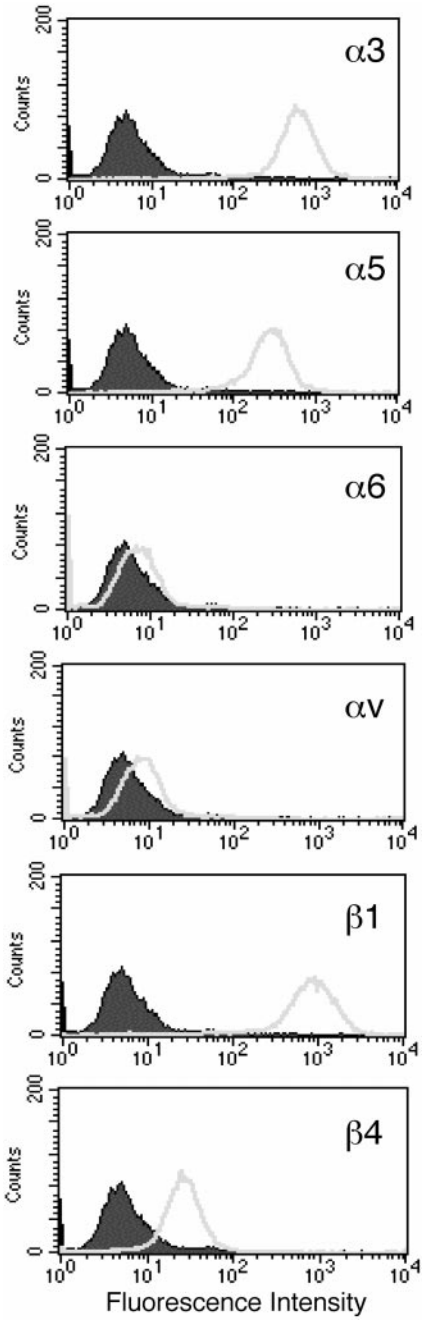

FIG. 1. **Flow cytometric analyses of integrin subunits on A549 cells.** A549 cells were incubated with mAbs specific to α_3, α_5, α_6, α_v, β_1, or β_4 integrin subunits and then stained with FITC-conjugated secondary antibody for flow cytometric analysis. The expression of each integrin subunit is shown as a *gray line*. The *black area* indicates the negative control following incubation with mouse IgG.

velopment and establishment of tissue architecture. Recently, we purified laminin-10/11 (LN-10/11) from the conditioned medium of A549 human lung carcinoma cells to find that the $\alpha_3\beta_1$ integrin is the preferred receptor for LN-10/11, although $\alpha_6\beta_1$ integrin serves as another LN-10/11 receptor in fibroblastic cells (16, 17). The mechanisms governing cell behavior on LN-10/11 and the signals transduced by $\alpha_3\beta_1$ and other cognate integrins, however, remain unclear.

In the present study, we examined the integrin-mediated signaling events resulting from adhesion to LN-10/11, compared against those from FN. LN-10/11 preferentially activate Rac, but not Rho, through an $\alpha_3\beta_1$ integrin-dependent pathway involving a $p130^{Cas}$-CrkII-DOCK180 complex, thereby strongly promoting cell migration through enhanced lamellipodia formation. FN, however, preferentially activates Rho, leading to enhanced stress fiber and focal contact formation.

EXPERIMENTAL PROCEDURES

Cells and Cell Culture—A549 human lung adenocarcinoma cells and ECV304 human endothelia-derived cells were maintained in Dulbecco's modified Eagle's medium (DMEM) supplemented with 10% fetal bovine serum (FBS) at 37 °C in a humidified atmosphere containing 5% CO_2. The MKN45 human gastric carcinoma cells were grown in RPMI 1640 containing 10% FBS.

Reagents and Antibodies—Monoclonal antibodies (mAbs) against Rac, CrkII, phosphotyrosine (PY20), paxillin, FAK, and the horseradish peroxidase-conjugated, anti-phosphotyrosine (RC20) antibodies were obtained from Transduction Laboratories (San Diego, CA). Polyclonal antibodies against $p130^{Cas}$, DOCK180, and Rho were purchased from Santa Cruz Biotechnology (Santa Cruz, CA). The mAb against the human α_6 integrin subunit (GoH3) was obtained from Cosmo Bio (Tokyo, Japan). mAbs against integrin α_v and β_4 (ASC-8) were purchased from Telios Pharmaceuticals (San Diego, CA) and Chemicon (Temecula, CA), respectively. The mAbs against α_3 (3G8), α_5 (5G10), and β_1 (4G2) integrins were produced and characterized in our laboratory (16, 18). F-actin was detected by rhodamine-labeled phalloidin obtained from Molecular Probes (Eugene, OR). The FITC-conjugated rabbit secondary antibody to mouse IgG was purchased from Cappel (West Chester, PA).

Preparation of LN-10/11 and LN-5—LN-10/11 were purified to homogeneity from conditioned media of A549 cells as described previously (16). The 5D6 mAb, recognizing human laminin α_5 chain, was used for immunoaffinity chromatography (19). Silver staining and immunoblotting with a panel of mAbs specific for individual laminin α chains verified that the purified LN-10/11 lacked other laminin isoforms (19). LN-5 was purified from the conditioned media of MKN45 cells by immunoaffinity chromatography using an anti-laminin γ_2 chain antibody (20).

Expression Plasmids—The pcDNA-CrkII expression plasmid, generated by transferring the CrkII cDNA insert from pCEFL-GST-CrkII to pcDNA-3.1 after *Bam*HI and *Not*I digestion, was the gift of Drs. Takahisa Takino and Kenneth Yamada (NIDCR, National Institutes of Health). The CrkII N-terminal SH3 mutant (CrkII-SH3M) and SH2 mutant (CrkII-SH2M) were generated by the substitution of leucine for tryptophan 169 and arginine 38, respectively, using the QuikChange™ site-directed mutagenesis kit (Stratagene, La Jolla, CA). The expression plasmid for the dominant-negative Rac^{Asn-17} was kindly provided by Dr. Kenneth Yamada (NIDCR, National Institutes of Health). The puromycin resistance plasmid pHA262pur was provided by Dr. Hein te Riele (The Netherlands Cancer Institute, Amsterdam). The expression plasmids for GST-RB (a fusion protein of glutathione *S*-transferase to the Rho-binding domain of bovine Rho kinase) and GST-CRIB (a fusion protein of glutathione *S*-transferase to the Cdc42/Rac interactive-binding domain of PAK1) were kindly provided by Dr. Kozo Kaibuchi (Nara Institute of Science and Technology, Japan).

Transfection and Selection—Thirty μg of each expression plasmid were co-transfected with 5 μg of pHA262Puro into 3×10^6 A549 cells by electroporation at 170 V and 960 microfarads with a Bio-Rad Gene Pulser. To increase expression of transfected genes, 5 mM sodium butyrate was included in the culture media. Cells were subcultured at a 1:3 dilution 12 h after transfection and maintained for 48 h in 1 μg/ml puromycin-containing medium. Before use, cells were cultured overnight in the absence of puromycin.

Flow Cytometry—Flow cytometric analysis was performed as described previously (20). Suspended A549 cells were incubated with anti-integrin mAbs (anti-α_3, α_5, α_6, α_v, β_1, and β_4) for 30 min at 4 °C. Following washing, cells were incubated with FITC-labeled secondary antibody for 30 min at 4 °C. Cells were then analyzed on a FACScan flow cytometer (Becton Dickinson, San Jose, CA).

Immunoprecipitation and Western Blotting—Twenty four hours after serum starvation, A549 cells with or without transfected plasmids were detached from culture flasks by treatment with 0.05% trypsin/EDTA, washed with serum-free DMEM containing 1% bovine serum albumin (BSA), and resuspended in the same medium. Cells were kept in suspension for 60 min at 37 °C on a rotator. 2×10^6 cells were allowed to spread on 60-mm tissue culture dishes coated with 5 nM of LN-10/11 or 20 nM of FN for 30 min. Following washing in ice-cold phosphate-buffered saline (PBS), cells were solubilized in 600 μl of 1% Triton lysis buffer (20 mM Tris-HCl, pH 7.5, 150 mM NaCl, 1 mM EDTA, 1 mM EGTA, 2.5 mM sodium pyrophosphate, 1 mM β-glycerophosphate, 1 mM sodium vanadate, 10 μg/ml leupeptin, 10 μg/ml aprotinin, 1 mM phen-

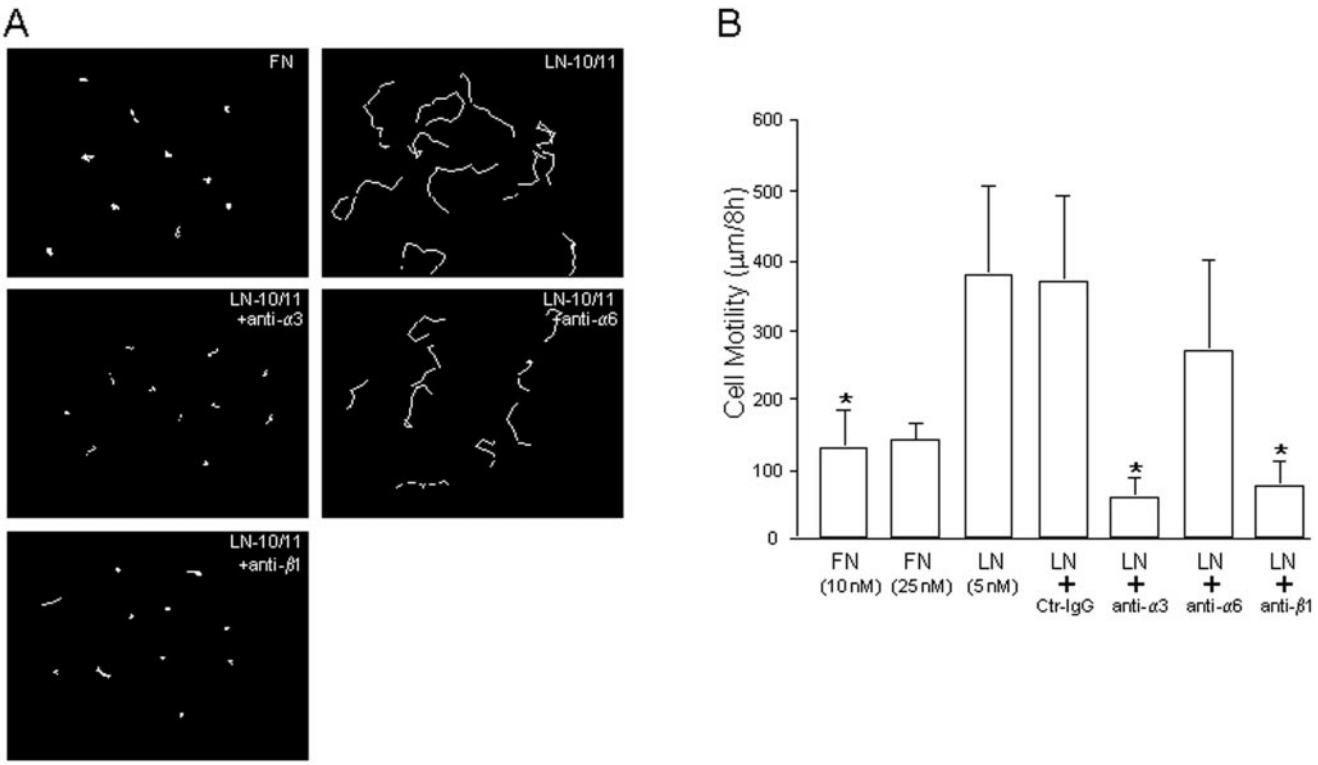

FIG. 2. **Migration of A549 cells on LN-10/11 is mediated by $\alpha_3\beta_1$ integrin.** A549 cells were replated on dishes coated with FN (10 or 25 nM) or LN-10/11 (5 nM) in the presence of 1% FBS and anti-integrin antibodies (10 μg/ml). Cell movements were monitored by time-lapse video microscopy. Cell motility was evaluated by velocity (μm/8 h), determined using Image-Pro software as described under "Experimental Procedures." Antibodies used were anti-α_3, -α_6, or -β_1 mAbs as well as control mouse IgG. *A*, representative paths of cell movements on LN-10/11 (5 nM) or FN (10 nM) tracked at 20-min intervals over a span of 8 h. *B*, quantification of cell motility as expressed as the mean ± S.D. in triplicate assays. Statistical analysis was performed using Student's *t* test. *, $p < 0.01$; **, $p < 0.001$; ***, $p > 0.05$.

ylmethylsulfonyl fluoride). The cell lysates were clarified by centrifugation at 20,000 × *g* for 15 min at 4 °C. Proteins were then immunoprecipitated from the lysates using a combination of 3 μg of specific mAbs and protein A-Sepharose beads. Immunoprecipitates were suspended in reducing or nonreducing sample buffer, heated to 100 °C for 3 min, resolved on 8 or 10% SDS-polyacrylamide gels, and electrophoretically transferred to nitrocellulose membranes. Immunoblots for phosphotyrosine, FAK, $p130^{Cas}$, CrkII, DOCK180, or other epitopes were visualized by ECL (Amersham Pharmacia Biotech).

Detection of GTP-loaded Rho and Rac—A549 cells were serum-starved overnight, detached in trypsin/EDTA, and kept in suspension in DMEM with 1% BSA for 90 min. Cells were plated on dishes coated with indicated concentrations of LN or FN. At the times indicated, cells were washed with ice-cold PBS and then lysed in buffer containing 1% Nonidet P-40, 50 mM Tris-HCl, pH 7.4, 100 mM NaCl, 10 mM $MgCl_2$, 1 mM dithiothreitol, 10 μg/ml leupeptin, 10 μg/ml aprotinin, and 1 mM phenylmethylsulfonyl fluoride. Lysates were clarified by centrifugation at 20,000 × *g* for 15 min at 4 °C and then incubated with either 30 μg of GST-CRIB or GST-RB for 60 min at 4 °C with 30 μl of glutathione-agarose beads. The immunoprecipitates were washed three times with lysis buffer, and then resolved on 12% SDS-polyacrylamide gels. Following electrophoretic transfer to nitrocellulose, the membranes were immunoblotted using anti-Rac mAb or polyclonal anti-Rho antibody. Whole cell lysates were also directly immunoblotted for the levels of total Rac or Rho for normalization.

Cell Motility Assays—A549 cells were replated on 50-mm glass microwell dishes (Matsunami, Co., Osaka, Japan) coated with either LN-10/11 (5 nM) or FN (20 nM) in serum-free DMEM and blocked with 1% BSA. Thirty minutes post-replating, the medium was changed to that containing 1% FBS with or without 10 μg/ml antibodies as indicated. Cell migration was then monitored using a Zeiss S-25 inverted microscope. Video images were collected with a CCD camera at 20-min intervals using the Image-Pro software (Media Cybernetics, Silver Springs, MD). The positions of nuclei were tracked to quantify cell motility. Velocities were calculated in micrometers per 8 h using the same software.

Immunofluorescence Microscopy—Glass coverslips were coated with LN (10 nM) or FN (40 nM) in PBS overnight at 4 °C and then blocked with 1% BSA. A549 cells were serum-starved overnight and then replated on the coverslips by incubating for 1 h in DMEM containing 1% BSA. Cells were then fixed with 3.7% paraformaldehyde in PBS for 20 min and permeabilized with 0.5% Triton X-100 for 5 min. Focal adhesions were visulized by incubating cells with mouse anti-paxillin antibody, following an incubation with FITC-conjugated rabbit antibody specific for mouse IgG. Actin filaments were stained with rhodamine-conjugated phalloidin.

RESULTS

LN-10/11 Stimulate Cell Migration via $\alpha_3\beta_1$ Integrin—Our previous studies demonstrate that LN-10/11 are very potent cell-adhesive proteins capable of utilizing both $\alpha_3\beta_1$ and $\alpha_6\beta_1$ integrins as major surface receptors (17). The adhesion of A549 cells onto LN-10/11, however, depends predominantly on $\alpha_3\beta_1$ integrin (16). This apparent discrepancy is due to the marginal expression level of $\alpha_6\beta_1$ integrin in A549 cells, as opposed to a high expression level of $\alpha_3\beta_1$ integrin (Fig. 1). Integrin $\alpha_5\beta_1$, the major receptor for FN, was expressed at lower levels than $\alpha_3\beta_1$ on A549 cells. Consistent with the relative expression of $\alpha_3\beta_1$ and $\alpha_5\beta_1$ integrins, the maximal level of A549 cell adhesion was attained at lower coating concentrations of LN-10/11 than FN (16). In our cell adhesion assays, the degree of A549 cell adhesion to substrates was comparable and close to the maximal level when coated with either 5 nM LN-10/11 or 20 nM FN. Unless otherwise specified, therefore, we have compared cellular responses to LN-10/11 and FN at these coating concentrations.

We compared the activity of LN-10/11 and FN to promote cell migration using time-lapse video microscopy (Fig. 2). The migration of A549 cells was significantly faster on LN-1oin the migration of A549 cells on LN-10/11, we examined the effects of function-blocking antibodies against α_3, α_6, and β_1 integrin chains on A549 cell migration. Anti-α_3 and anti-β_1 antibodies, but not anti-α_6 antibody, inhibited cell migration on LN-10/11

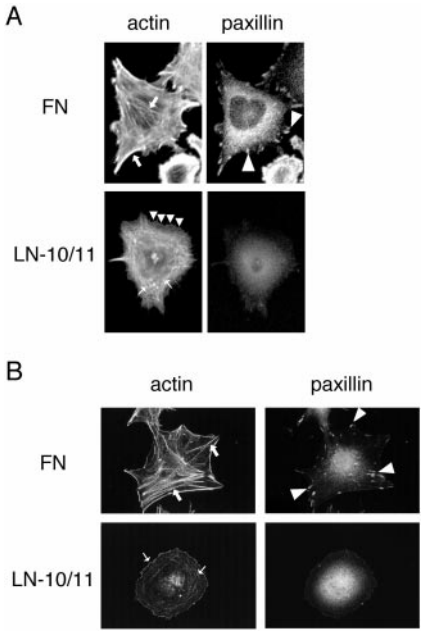

FIG. 3. **Cytoskeletal reorganization and focal contact formation in the presence of LN-10/11 or FN.** Serum-starved A549 cells (*A*) or ECV304 cells (*B*) were allowed to spread on coverslips coated with FN (20 nM; *upper panels*) or LN-10/11 (10 nM; *lower panels*) for 1 h in DMEM containing 1% BSA. Cells were then stained with rhodamine-phalloidin to detect F-actin (*left*) or anti-paxillin antibody to detect focal adhesions (*right*). The *thick* and *thin arrows* specify stress fibers and short actin filaments, respectively. The *large* and *small arrowheads* designate focal contacts and membrane ruffles, respectively.

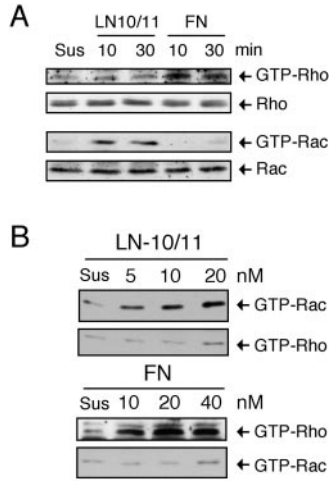

FIG. 4. **Differential activation of Rho and Rac on LN-10/11 and FN.** *A*, serum-starved A549 cells were detached and held in suspension for 90 min and then replated on dishes coated with LN-10/11 (5 nM) or FN (20 nM) for 10 or 30 min. Cell lysates were incubated with GST-RB or GST-CRIB immobilized on agarose beads. GTP-loaded Rho and Rac were detected by Western blotting (*upper panels*). Total cell lysates were also probed for Rho or Rac to demonstrate equal amounts of total protein (*lower panel*). *B*, serum-starved cells were replated on dishes coated with different concentrations of LN-10/11 or FN for 30 min. The levels of GTP-loaded and total Rho and Rac were detected as described above. *Sus*, cells kept in suspension. The results shown are representative of three independent experiments.

(Fig. 2). These results were consistent with previous observations that the attachment of A549 cells on LN-10/11 was inhibited by anti-α_3, but not anti-α_6, antibodies (16). The adhesive interaction of A549 cells with LN-10/11, therefore, is largely dependent on $\alpha_3\beta_1$ integrin.

LN-10/11 Do Not Induce the Formation of Stress Fibers and Focal Contacts—To explore differences in signals transduced from LN-10/11 and FN, we examined the reorganization of the actin cytoskeleton and the formation of focal contacts in A549 cells adhering to either LN-10/11 or FN. Actin reorganized into microfilament bundles in cells spread on FN, although the cells plated on LN-10/11 contained short, thin actin filaments forming lamellipodia at the cell periphery (Fig. 3*A*). Clear focal contacts, visualized using an anti-paxillin antibody, were detected in cells spread on FN but not on LN-10/11. We extended this observation to other cell types by examining the actin cytoskeleton and focal contact formation in ECV304 cells (Fig. 3*B*). These cells, when adhered to FN, demonstrated well organized actin stress fibers and clear focal contacts; cells spread on LN-10/11 contained thin, short actin filaments arranged circumferentially without clear focal contacts.

LN-10/11 and FN Differentially Regulate Rac and Rho Activation—Cytoskeletal reorganization associated with cell spreading is regulated by the Rho family of small GTPases. Rho activation controls the assembly of stress fibers and focal adhesions; activation of Cdc42 and Rac results in the formation of filopodia and lamellipodia, respectively (21). To examine the differential activation of Rac and Rho by LN-10/11 and FN, the quantities of GTP-loaded Rac and Rho were determined by pull-down assays, based on their specific binding to the GST-CRIB (a fusion protein containing the Cdc42/Rac-binding domain of PAK1) and GST-RB (a fusion protein containing Rho-binding domain of Rho kinase). Serum-starved A549 cells were detached and kept in suspension for 90 min and then replated on either LN-10/11 or FN-coated dishes. The level of GTP-bound Rho was significantly elevated on FN as early as 10 min (Fig. 4*A*). Only a marginal increase in the level of GTP-Rho was observed in cells adhering to LN-10/11. In contrast, a significant increase in Rac activation was observed in cells adhering to LN-10/11, not FN. The complementary profiles of Rho and Rac activation on FN and LN-10/11 were preserved even at higher ligand coating concentrations (Fig. 4*B*), indicating that signals transduced from FN and LN-10/11 are distinct in their activation of Rho family GTPases.

LN-10/11 Preferentially Phosphorylate p130^{Cas}—The activation of integrins upon cell adhesion to the ECM leads to an increase in the phosphorylation of FAK and p130^{Cas} (22). To explore the differences in the signaling pathways mediated by LN-10/11 and FN, we examined the phosphorylation of FAK and p130^{Cas} in A549 cells plated on either FN, LN-10/11, or LN-5. LN-5 was included as a control ligand binding to $\alpha_3\beta_1$ integrin (20, 23). Although the phosphorylation of FAK and p130^{Cas} increased in cells adhering to these proteins, FAK phosphorylation levels were much higher on FN than on LN-10/11 or LN-5 (Fig. 5*A*). Conversely, the level of p130^{Cas} phosphorylation was higher on LN-10/11 and LN-5 than on FN (Fig. 5*B*). Densitometric analysis demonstrated that the ratio of phosphorylated FAK to phosphorylated p130^{Cas} in the cells spread on FN was two times greater than in cells plated on either LN-10/11 or LN-5 (Fig. 5*C*), suggesting that LN-10/11 and FN activate distinct integrin-mediated signaling pathways.

LN-10/11 Enhance Formation of the p130^{Cas}-CrkII-DOCK180 Complex—The association of p130^{Cas} with the adaptor protein CrkII is important in cell migration over the ECM (5). Tyrosine phosphorylation promotes the coupling of p130^{Cas} to CrkII, in turn coupling to downstream effectors such as DOCK180 (6). To determine whether the increased p130^{Cas} phosphorylation on LN-10/11 is associated with increased formation of the p130^{Cas}-CrkII-DOCK180 complex and subsequent Rac activation, we transfected either the wild-type CrkII or its N-terminal SH3 mutant form (CrkII-SH3M) together with the puromycin selection plasmid into A549 cells. The

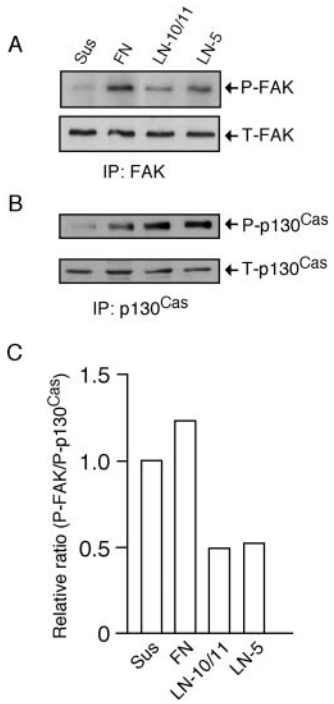

FIG. 5. **Differential phosphorylation of FAK and p130^{Cas} on LN-10/11 and FN.** Serum-starved A549 cells were detached and held in suspension for 60 min and then replated on the dishes coated with LN-10/11 (5 nM) or FN (20 nM) for 30 min. Cell lysates were immunoprecipitated with antibodies against FAK (*A*) or p130^{Cas} (*B*). Immunoprecipitates were then immunoblotted with either anti-phosphotyrosine antibody to detect phosphorylated FAK (*P-FAK*) and p130^{Cas} (*P-p130^{Cas}*) or anti-FAK and anti-p130^{Cas} antibodies to detect total FAK (*T-FAK*) and total p130^{Cas} (*T-p130^{Cas}*), respectively. *Sus*, cells kept in suspension. *C,* the ratios of phosphorylated FAK to phosphorylated p130^{Cas} were determined by densitometry of the bands on immunoblots after normalization against the band intensities of total FAK and p130^{Cas}. The data are expressed as relative values after normalization against the ratio in the cells in suspension. The results shown are representative of two independent experiments.

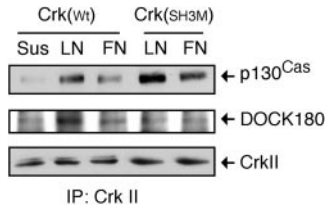

FIG. 6. **Effects of LN-10/11 and FN on p130^{Cas}-CrkII-DOCK180 complex formation.** A549 cells were co-transfected with pHA262pur and plasmids encoding either wild-type CrkII (*Wt*) or CrkII N-terminal SH3 mutant (*SH3M*). After selection with puromycin for 2 days, cells were serum-starved overnight in 0.2% FBS, detached, and held in suspension for 60 min. Cells were either kept in suspension (*Sus*) or replated on the dishes coated with LN-10/11 (5 nM) or FN (20 nM) for 30 min. CrkII was immunoprecipitated (*IP*) from cell lysates utilizing an anti-CrkII antibody, and the precipitates were detected by immunoblotting with an anti-p130^{Cas} (*top*), anti-DOCK180 (*middle*), or anti-CrkII (*bottom*) antibody. The data shown are representative of two independent experiments.

mutant CrkII is defective in the coupling to downstream effectors. After selection with puromycin for 2 days, the surviving cells were starved in medium containing 0.2% serum for 24 h. CrkII was immunoprecipitated from cell lysates with anti-CrkII, followed by immunoblotting with either anti-p130^{Cas} or anti-DOCK180. In wild-type CrkII transfectants, both p130^{Cas} and DOCK180 were associated with CrkII in cells adhering to LN-10/11 (Fig. 6). Only marginal amounts of p130^{Cas} and DOCK180 were associated with CrkII in cells adhering to FN, suggesting that LN-10/11 preferentially enhance the formation of the p130^{Cas}-CrkII-DOCK180 complex. Consistent with these results, DOCK180 was not immunoprecipitated in association with CrkII from cells expressing the CrkII SH3 mutant, even though the association of p130^{Cas} with CrkII was unaffected. These results confirm that the N-terminal SH3 domain of CrkII is essential for DOCK180 binding (6).

Overexpression of CrkII SH3 Mutant Inhibits Rac Activation on LN-10/11—DOCK180 activates Rac through binding to the CrkII-p130^{Cas} complex (6). The CrkII SH3 mutant cannot associate with DOCK180; therefore, we examined the inhibition of Rac activation by the CrkII SH3 mutant upon plating transfected cells on LN-10/11. The levels of GTP-bound Rac in the presence of LN-10/11 were elevated in cells transfected with wild-type CrkII; this activation was blocked in cells transfected with the CrkII SH3 mutant (Fig. 7, *A* and *C*). In contrast, Rho activation after plating cells on FN was not affected by expression of the CrkII SH3 mutant (Fig. 7, *B* and *D*). These results suggest that, in A549 cells, LN-10/11 activate Rac through the p130^{Cas}-CrkII-DOCK180 pathway.

Overexpression of CrkII SH3 or SH2 Mutants Inhibits Cell Migration on LN-10/11—To confirm the involvement of CrkII in cell migration on LN-10/11-coated substrates, A549 cells were transfected with either a dominant-negative Rac (Rac^{Asn-17}) or CrkII SH2 and SH3 mutants, each defective in coupling to p130^{Cas} or DOCK180, respectively. We measured the migration of these transfectants over LN-10/11-coated substrates using time-lapse video microscopy. Under the condition where the levels of expression of wild-type and mutant CrkII were comparable and 4–6-fold greater than that of endogenous CrkII (Fig. 8*B*), transfection of either the CrkII SH2 or SH3 mutant reduced cell migration to 50 and 53% of control cells transfected with a puromycin resistance plasmid alone, respectively, although transfection of wild-type CrkII had little effect on cell migration (Fig. 8*A*). Incomplete inhibition of cell migration by transfection of CrkII SH2 or SH3 mutants may result from the presence of other signaling pathways regulating integrin- and growth factor-mediated cell migration like the mitogen-activated protein kinase pathways (24, 25). Overexpression of a dominant-negative Rac also reduced cell migration on LN-10/11 to 45% of control cells, confirming that Rac activation plays a crucial role in cell migration over LN-10/11.

DISCUSSION

In this study, we explored the mechanisms of cell spreading and migration over LN-10/11 with an emphasis on integrin-mediated signaling pathways. By using transfection of wild-type or dominant-negative signaling molecules together with biochemical analyses, we found that LN-10/11 and FN have distinct effects on cell spreading and migration as summarized in Fig. 9. LN-10/11 induce the formation of protrusive structures such as membrane ruffles and lamellipodia; FN enhances the formation of actin stress fibers and focal contacts. Consistent with these morphological distinctions, LN-10/11 are more potent than FN in promoting cell migration. LN-10/11 preferentially activate Rac, not Rho, whereas Rho, not Rac, is activated by FN. Rac activation is required for cell migration on LN-10/11, since cell migration is down-regulated in cells overexpressing a dominant-negative Rac^{Asn-17}. Rac activation on LN-10/11 is mediated by the p130^{Cas}-CrkII-DOCK180 pathway since (*a*) p130^{Cas} is preferentially tyrosine-phosphorylated in cells adhering to LN-10/11 as compared with cells adhering to FN; (*b*) the association of CrkII with p130^{Cas} and DOCK180 is enhanced in cells adhering to LN-10/11, not FN; and (*c*) LN-10/11-mediated Rac activation is abolished by overexpression of a CrkII SH3 mutant. Both CrkII SH2 and SH3 mutants, as well as Rac^{Asn-17}, inhibit cell migration on LN-10/11, indicating

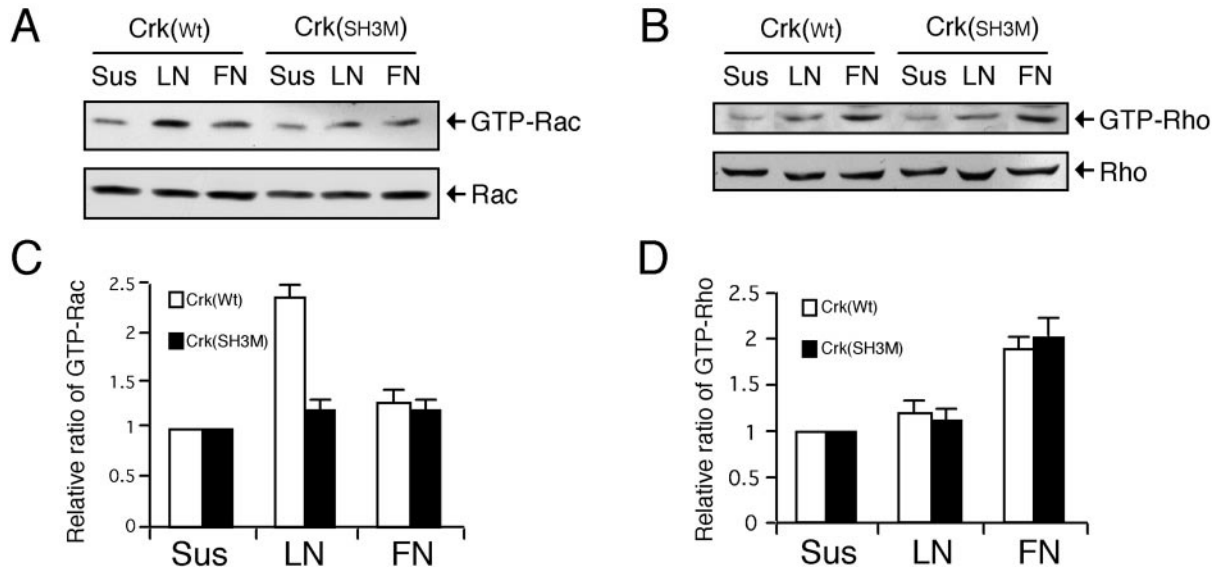

FIG. 7. **Overexpression of the CrkII SH3 mutant inhibits Rac activation on LN-10/11-coated substrates.** A549 cells, transfected with either wild-type CrkII (*Wt*) or CrkII SH3 mutant (*SH3M*) were selected with puromycin as described in Fig. 6. Serum-starved transfectants were detached, held in suspension for 60 min, and then either kept in suspension (*Sus*) or replated on dishes coated with LN-10/11 (5 nM) or FN (20 nM) for 30 min. Cell lysates were incubated with either GST-CRIB or GST-RB immobilized on glutathione-agarose beads. Bound GTP-loaded Rac and Rho were detected by immunoblotting with anti-Rac (*A*) or Rho (*B*) antibodies (*upper panels*). Cell lysates were also directly probed for total Rac or Rho (*lower panels*). The intensities of the bands of GTP-loaded Rac (*C*) and Rho (*D*) relative to those of total Rac/Rho were quantified by densitometry. The data shown represent the mean ± S.E. of two independent experiments, expressed as relative values after normalization against the ratio in the cells kept in suspension.

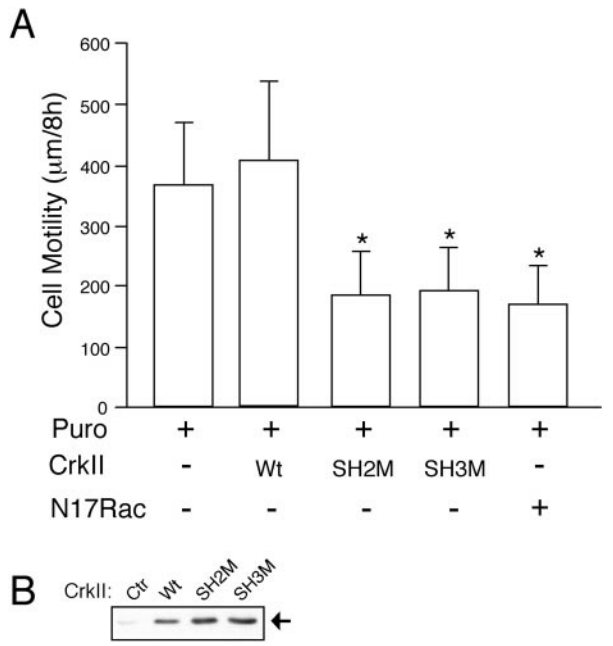

FIG. 8. **Overexpression of CrkII SH2 and SH3 mutants inhibits cell motility.** A549 cells were co-transfected with pHA262pur and plasmids encoding either the wild-type CrkII (*Wt*), CrkII SH2 mutant (*SH2M*), CrkII N-terminal SH3 mutant (*SH3M*), or dominant-negative Rac (*N17Rac*). Transfectants, selected with puromycin (*Puro*), were replated on dishes coated with LN-10/11. Cell movements were monitored by time-lapse video microscopy. *A*, cell motility, determined using Image-Pro software, was expressed as velocity (μm/8 h). Data shown are the mean ± S.D. from three independent experiments. Statistical analysis was performed using Student's *t* test. *, $p < 0.01$ *versus* control. *N17Rac*, $Rac^{Asn\text{-}17}$. *B*, the expression levels of wild-type or mutant CrkII were detected by immunoblotting with anti-CrkII antibody. *Ctr*, cells transfected with pHA262pur alone.

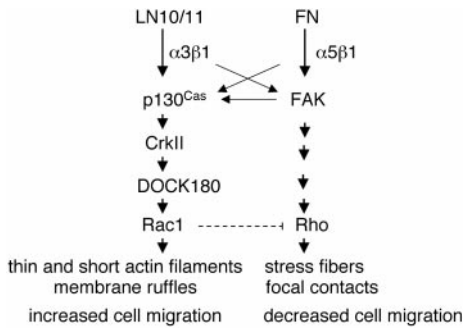

FIG. 9. **Proposed schemes of the integrin-mediated signaling pathways differentially activated by LN-10/11 and FN.** Engagement of $\alpha_3\beta_1$ and $\alpha_5\beta_1$ integrins with LN-10/11 or FN induces differential tyrosine phosphorylation of FAK and $p130^{Cas}$, activating distinct downstream signaling pathways, featuring distinctive activation of Rho and Rac. Our results indicate that $\alpha_3\beta_1$ integrin-mediated signals preferentially activate Rac through the $p130^{Cas}$-CrkII-DOCK180 pathway, whereas $\alpha_5\beta_1$ integrin-mediated signals lead to Rho activation via an undefined pathway. Recently, Rac activation has been shown to down-regulate Rho activity (*dashed line*; see Refs. 43–45).

that LN-10/11 promote cell migration by preferential activation of Rac through the $p130^{Cas}$-CrkII-DOCK180 pathway.

Different Signals are Transduced by $\alpha_3\beta_1$ and $\alpha_5\beta_1$ Integrins—Ligand binding to integrins activates intracellular signaling cascades, which regulate various cellular functions including cytoskeletal organization and cell proliferation and differentiation. Up to 25 integrin $\alpha\beta$ heterodimers have been identified; the $\alpha_5\beta_1$ integrin has been most extensively studied as a model for integrin signaling through its specific interaction with FN, a well characterized ECM ligand containing an RGD motif. Many integrin-mediated signaling events, including tyrosine phosphorylation of FAK, $p130^{Cas}$, paxillin, and other adapter proteins, activation of the Rho family of small GTPases, and activation of mitogen-activated protein kinases and subsequent cell cycle progression, have been elucidated in cells adhering to FN through $\alpha_5\beta_1$ integrin (2, 22, 26). Despite extensive studies of signaling events involving $\alpha_5\beta_1$ and other integrins recognizing an RGD motif, little is known about signaling through RGD-independent integrins, particularly those recognizing LNs. Signals transduced from LN-1 and FN through $\alpha_6\beta_1$ and $\alpha_5\beta_1$ integrins, respectively, are likely to antagonistically regulate cell proliferation and differentiation.

FN suppresses differentiation to promote the proliferation of myoblasts, whereas LN-1 has the opposite effect (27). Consistent with this observation, transfection of the cytoplasmic domain of α_6 integrin subunit promotes myoblast differentiation, whereas transfection of the cytoplasmic domain of α_5-subunit suppresses differentiation and promotes proliferation (28). $\alpha_3\beta_1$ integrin may also transduce signals antagonistic against those from $\alpha_5\beta_1$ and other integrins, as the ablation of $\alpha_3\beta_1$ integrin from epithelial cells results in an enhanced formation of stress fibers and focal contacts (29, 30), suggesting that $\alpha_3\beta_1$ integrin transduces a signal that trans-dominantly inhibits the cytoskeletal reorganization induced by other integrins. The molecular mechanism underlying these phenomena, however, has not been addressed in depth. Our results clearly show that the signaling pathway activated by $\alpha_3\beta_1$ integrin is distinct from that activated by $\alpha_5\beta_1$ integrin with respect to the phosphorylation of FAK and $p130^{Cas}$, the coupling of CrkII with $p130^{Cas}$ and DOCK180, and the activation of Rac and Rho, resulting in enhanced cell migration on LN-10/11 with a concomitant suppression of stress fiber and focal contact formation. This is the first report demonstrating a clear distinction in signaling events elicited by $\alpha_3\beta_1$ and $\alpha_5\beta_1$ integrins.

Activation of Rho Family GTPases Is Substrate-dependent—Most studies of ECM-dependent activation of Rho family GTPases have been performed on fibroblasts (*e.g.* Swiss or NIH 3T3 fibroblasts) adhering to FN. FN activates Rho (31, 32) as well as Rac and Cdc42 (33, 34), although most studies do not examine both Rho and Rac/Cdc42 activation in the same cell system. Our data demonstrate that, in A549 cells, LN-10/11 preferentially activate Rac, whereas FN activates Rho. As the adhesion of A549 cells to LN-10/11 and FN is mediated by $\alpha_3\beta_1$ and $\alpha_5\beta_1$ integrins, respectively, our results indicate that different integrins transduce signals differentially activating the Rho family of GTPases. Recently, Wenk *et al.* (32) reported that tenascin-C suppresses the activation of Rho and subsequent stress fiber formation in cells plated on three-dimensional fibrin-FN matrix, again suggesting the substrate-dependent activation of Rho family GTPases.

Signaling pathways activating Rho family GTPases and their downstream effectors may vary considerably among different cell types. Constitutively active Rac is sufficient to induce membrane ruffles in Swiss 3T3 and NIH 3T3 fibroblasts (3), although both the Rac-mediated pathway and the phosphorylation of adducin by the Rho/Rho kinase pathway is required for 12-*O*-tetradecanoylphorbol-13-acetate-induced membrane ruffling in Madin-Darby canine kidney epithelial cells (35). In epithelial cells, $p120^{Ctn}$, a putative negative regulator of cadherin-mediated cell-cell adhesion, inhibits Rho activation when present as a cadherin-unbound form (36, 37), supporting the possibility that signaling pathways regulating the activation of Rho family GTPases differ in epithelial cells from those in fibroblasts.

LN-10/11 Stimulate Cell Migration via $p130^{Cas}$-CrkII-DOCK180-Rac Pathway—The dominant-negative form of Rac (Rac^{Asn-17}) blocks integrin-mediated cell migration (5, 7), linking Rac activation to cell migration. To explore the mechanism underlying cell migration over LN-10/11, we examined the tyrosine phosphorylation state of FAK and $p130^{Cas}$, molecules implicated in signaling events promoting cell migration (38). $p130^{Cas}$ is preferentially tyrosine-phosphorylated on LN-10/11, whereas FAK is more phosphorylated on FN than on LN-10/11, suggesting the involvement of $p130^{Cas}$ tyrosine phosphorylation in LN-10/11-driven cell migration. Tyrosine phosphorylation of $p130^{Cas}$ has also been implicated as a critical event in the migration and invasion of tumor cells. Pancreatic carcinoma cells selected for high migration *in vitro* exhibited increased tyrosine phosphorylation of $p130^{Cas}$ (5). Transfection of wild-type $p130^{Cas}$ is sufficient to promote tumor cell migration; a non-phosphorylatable $p130^{Cas}$ mutant lacking the substrate domain cannot mediate this effect (5). Similar results were also obtained with COS cells transfected with either wild-type or the substrate domain-deficient mutant of $p130^{Cas}$ (7). Tyrosine phosphorylation of the substrate domain of $p130^{Cas}$ is dependent on both FAK and Src family kinases, the latter serving as the major kinases phosphorylating the substrate domain, whereas the former serving as a template for the assemblage of a ternary complex consisting of FAK, $p130^{Cas}$, and Src kinases (8, 39). Disruption of this ternary complex by overexpression of FAK mutants defective in either Src kinase binding or $p130^{Cas}$ binding, as well as by overexpression of the $p130^{Cas}$ SH3 domain competing with endogenous $p130^{Cas}$ for FAK binding, has been shown to suppress integrin-mediated cell migration (40, 41). In addition, cells derived from either $p130^{Cas}$-deficient or Src/Yes/Fyn triple-deficient mouse embryos are significantly less motile than wild-type cells (8, 42), supporting the importance of the tyrosine phosphorylation of $p130^{Cas}$ in cell migration.

The coupling of $p130^{Cas}$ to CrkII may serve as a molecular switch for induction of cell migration through Rac activation (5, 7, 41). Consistent with this view, our data demonstrate that coupling of CrkII with $p130^{Cas}$ is increased in cells plated on LN-10/11, not FN. Increased formation of the $p130^{Cas}$-CrkII complex is accompanied by an increased association of DOCK180 with this complex, enhancing Rac activation. DOCK180 serves as the major guanine nucleotide exchange factor for Rac in integrin-dependent cell migration (6, 7). Rac activation also down-regulates Rho activity (43–45); the minimal Rho activation in cells adhering to LN-10/11 may result from enhanced Rac activation on LN-10/11.

Possible Mechanisms Directing the Signaling Pathways through Different Integrins—Our data suggest that LN-10/11 and FN differentially activate Rho family GTPases through distinct signaling pathways involving the $\alpha_3\beta_1$ and $\alpha_5\beta_1$ integrins. The mechanism directing the activation of individual signaling pathways specific to each integrin type remains unclear. Membrane proteins associating with a subset of integrins, such as transmembrane-4 superfamily proteins and caveolin-1 (46, 47), may control the activation of integrin type-specific signaling pathways. Many transmembrane-4 superfamily proteins associate with $\alpha_3\beta_1$, $\alpha_6\beta_1$, and some other β_1-containing integrins. CD151, selectively associated with $\alpha_3\beta_1$ in stringent detergents (48), is involved in integrin-mediated cell migration and invasion, as antibodies against CD151 inhibit the migration of neutrophils and endothelial cells (48, 49). In addition, a monoclonal antibody inhibiting the *in vivo* metastasis of human epidermoid carcinoma cells was found to be directed to CD151 (50). Given that the association of CD151 with $\alpha_3\beta_1$ integrin is highly stable and stoichiometric and that phosphatidylinositol 4-kinase is associated with the CD151-$\alpha_3\beta_1$ integrin complex (48), CD151 may specify the signaling pathways downstream of $\alpha_3\beta_1$ integrin. In contrast, caveolin-1, a membrane protein localizing to caveolae, associates with $\alpha_5\beta_1$ and other integrins, but not with $\alpha_3\beta_1$, resulting in the recruitment of Shc via activation of Fyn (47, 51). Although it is not clear if the association of transmembrane-4 superfamily proteins and/or caveolin-1 with integrin subsets directs the differential signaling events occurring on LN-10/11 and FN, further studies will shed a light on the molecular mechanisms operating in ECM-regulated, cellular behaviors in physiological and pathological conditions.

Acknowledgments—We thank Dr. Kozo Kaibuchi for supplying expression vectors for GST-CRIB and GST-RB. We also thank Drs. Ken-

neth Yamada and Takahisa Takino for providing the pcDNA-CrkII expression plasmids. We greatly appreciate the excellent assistance of Ryoko Nishiuchi and Kazuaki Minami in the purification of LN-10/11.

REFERENCES

1. Schwartz, M. A., Schaller, M. D., and Ginsberg, M. H. (1995) *Annu. Rev. Cell Dev. Biol.* **11,** 549–599
2. Yamada, K. M., and Miyamoto, S. (1995) *Curr. Opin. Cell Biol.* **7,** 681–689
3. Hall, A. (1998) *Science* **279,** 509–514
4. Schlaepfer, D. D., and Hunter, T. (1998) *Trends Cell Biol.* **8,** 151–157
5. Klemke, R. L., Leng, J., Molander, R., Brooks, P. C., Vuori, K., and Cheresh, D. A. (1998) *J. Cell Biol.* **140,** 961–972
6. Kiyokawa, E., Hashimoto, Y., Kobayashi, S., Sugimura, H., Kurata, T., and Matsuda, M. (1998) *Genes Dev.* **12,** 3331–3336
7. Cheresh, D. A., Leng, J., and Klemke, R. L. (1999) *J. Cell Biol.* **146,** 1107–1116
8. Klinghoffer, R. A., Sachsenmaier, C., Cooper, J. A., and Soriano, P. (1999) *EMBO J.* **18,** 2459–2471
9. Hynes, R. O. (1996) *Dev. Biol.* **180,** 402–412
10. Timpl, R. (1996) *Curr. Opin. Cell Biol.* **8,** 618–624
11. Aumailley, M., and Smyth, N. (1998) *J. Anat.* **193,** 1–21
12. Koch, M., Olson, P. F., Albus, A., Jin, W., Hunter, D. D., Brunken, W. J., Burgeson, R. E., and Champliaud, M. F. (1999) *J. Cell Biol.* **145,** 605–618
13. Miner, J. H., Cunningham, J., and Sanes, J. R. (1998) *J. Cell Biol.* **143,** 1713–1723
14. Miner, J. H., Lewis, R. M., and Sanes, J. R. (1995) *J. Biol. Chem.* **270,** 28523–28526
15. Sorokin, L. M., Pausch, F., Frieser, M., Kroger, S., Ohage, E., and Deutzmann, R. (1997) *Dev. Biol.* **189,** 285–300
16. Kikkawa, Y., Sanzen, N., and Sekiguchi, K. (1998) *J. Biol. Chem.* **273,** 15854–15859
17. Kikkawa, Y., Sanzen, N., Fujiwara, H., Sonnenberg, A., and Sekiguchi, K. (2000) *J. Cell Sci.* **113,** 869–876
18. Manabe, R., Ohe, N., Maeda, T., Fukuda, T., and Sekiguchi, K. (1997) *J. Cell Biol.* **139,** 295–307
19. Fujiwara, H., Kikkawa, Y., Sanzen, N., and Sekiguchi, K. (2001) *J. Biol. Chem.* **276,** 17550–17558
20. Fukushima, Y., Ohnishi, T., Arita, N., Hayakawa, T., and Sekiguchi, K. (1998) *Int. J. Cancer* **76,** 63–72
21. Nobes, C. D., and Hall, A. (1995) *Cell* **81,** 53–62
22. Clark, E. A., and Brugge, J. S. (1995) *Science* **268,** 233–239
23. Lampe, P. D., Nguyen, B. P., Gil, S., Usui, M., Olerud, J., Takada, Y., and Carter, W. G. (1998) *J. Cell Biol.* **143,** 1735–1747
24. Klemke, R. L., Cai, S., Giannini, A. L., Gallagher, P. J., de Lanerolle, P., and Cheresh, D. A. (1997) *J. Cell Biol.* **137,** 481–492
25. Gu, J., Tamura, M., Pankov, R., Danen, E. H., Takino, T., Matsumoto, K., and Yamada, K. M. (1999) *J. Cell Biol.* **146,** 389–403
26. Giancotti, F. G., and Ruoslahti, E. (1999) *Science* **285,** 1028–1032
27. von der Mark, K., and Ocalan, M. (1989) *Differentiation* **40,** 150–157
28. Sastry, S. K., Lakonishok, M., Thomas, D. A., Muschler, J., and Horwitz, A. F. (1996) *J. Cell Biol.* **133,** 169–184
29. Hodivala-Dilke, K. M., DiPersio, C. M., Kreidberg, J. A., and Hynes, R. O. (1998) *J. Cell Biol.* **142,** 1357–1369
30. Wang, Z., Symons, J. M., Goldstein, S. L., McDonald, A., Miner, J. H., and Kreidberg, J. A. (1999) *J. Cell Sci.* **112,** 2925–2935
31. Ren, X. D., Kiosses, W. B., and Schwartz, M. A. (1999) *EMBO J.* **18,** 578–585
32. Wenk, M. B., Midwood, K. S., and Schwarzbauer, J. E. (2000) *J. Cell Biol.* **150,** 913–920
33. Price, L. S., Leng, J., Schwartz, M. A., and Bokoch, G. M. (1998) *Mol. Biol. Cell* **9,** 1863–1871
34. del Pozo, M. A., Price, L. S., Alderson, N. B., Ren, X. D., and Schwartz, M. A. (2000) *EMBO J.* **19,** 2008–2014
35. Fukata, Y., Oshiro, N., Kinoshita, N., Kawano, Y., Matsuoka, Y., Bennett, V., Matsuura, Y., and Kaibuchi, K. (1999) *J. Cell Biol.* **145,** 347–361
36. Anastasiadis, P. Z., Moon, S. Y., Thoreson, M. A., Mariner, D. J., Crawford, H. C., Zheng, Y., and Reynolds, A. B. (2000) *Nat. Cell Biol.* **2,** 637–644
37. Noren, N. K., Liu, B. P., Burridge, K., and Kreft, B. (2000) *J. Cell Biol.* **150,** 567–580
38. O'Neill, G. M., Fashena, S. J., and Golemis, E. A. (2000) *Trends Cell Biol.* **10,** 111–119
39. Vuori, K., Hirai, H., Aizawa, S., and Ruoslahti, E. (1996) *Mol. Cell. Biol.* **16,** 2606–2613
40. Cary, L. A., Chang, J. F., and Guan, J. L. (1996) *J. Cell Sci.* **109,** 1787–1794
41. Cary, L. A., Han, D. C., Polte, T. R., Hanks, S. K., and Guan, J. L. (1998) *J. Cell Biol.* **140,** 211–221
42. Honda, H., Nakamoto, T., Sakai, R., and Hirai, H. (1999) *Biochem. Biophys. Res. Commun.* **262,** 25–30
43. Leeuwen, F. N., Kain, H. E., Kammen, R. A., Michiels, F., Kranenburg, O. W., and Collard, J. G. (1997) *J. Cell Biol.* **139,** 797–807
44. Rottner, K., Hall, A., and Small, J. V. (1999) *Curr. Biol.* **9,** 640–648
45. Sander, E. E., ten Klooster, J. P., van Delft, S., van der Kammen, R. A., and Collard, J. G. (1999) *J. Cell Biol.* **147,** 1009–1022
46. Hemler, M. E. (1998) *Curr. Opin. Cell Biol.* **10,** 578–585
47. Wary, K. K., Mariotti, A., Zurzolo, C., and Giancotti, F. G. (1998) *Cell* **94,** 625–634
48. Yauch, R. L., Berditchevski, F., Harler, M. B., Reichner, J., and Hemler, M. E. (1998) *Mol. Biol. Cell* **9,** 2751–2765
49. Yanez-Mo, M., Alfranca, A., Cabanas, C., Marazuela, M., Tejedor, R., Ursa, M. A., Ashman, L. K., de Landazuri, M. O., and Sanchez-Madrid, F. (1998) *J. Cell Biol.* **141,** 791–804
50. Testa, J. E., Brooks, P. C., Lin, J. M., and Quigley, J. P. (1999) *Cancer Res.* **59,** 3812–3820
51. Wary, K. K., Mainiero, F., Isakoff, S. J., Marcantonio, E. E., and Giancotti, F. G. (1996) *Cell* **87,** 733–743

Laminin-10/11 and Fibronectin Differentially Regulate Integrin- dependent Rho and Rac Activation via p130 ^{Cas}-CrkII-DOCK180 Pathway

Jianguo Gu, Yasuhiro Sumida, Noriko Sanzen and Kiyotoshi Sekiguchi

J. Biol. Chem. 2001, 276:27090-27097.
doi: 10.1074/jbc.M102284200 originally published online May 21, 2001
